Analysis of secretome changes uncovers an autocrine/paracrine component in the ability of c -Myc to modulate cell proliferation and motility

Pocsfalvi, G ; Votta, G ; De Vincenzo, A ; Fiume, I ; Raj, D A A ; Marra, Giancarlo ; Stoppelli, M P ; Iaccarino, I

Abstract: Proteins secreted by cancer cells are a major component of tumor microenvironment. However, little is known on the impact of single oncogenic lesions on the expression of secreted proteins at early stages of tumor development. Because c-Myc over-expression is among the most frequent alterations in cancer, here we investigated the effect of sustained c-Myc expression on the secretome of a non-transformed human epithelial cell line (hT-RPE). By using a quantitative proteomic approach we have identified 125 proteins in conditioned media of hT-RPE/MycER cells upon c-Myc induction. Analysis of the 49 proteins significantly down-regulated by c-Myc, revealed a marked enrichment of factors associated with growth inhibition and cellular senescence. Accordingly, media conditioned by hT-RPE cells expressing c-Myc show an increased ability to sustain hT-RPE cellular proliferation/viability. We also find a marked down-regulation of several structural and regulatory components of the extracellular matrix (ECM), which correlates with an increased chemotactic potency of the conditioned media towards fibroblasts, a major cellular component of tumor stroma. In accordance with these data, the expression of the majority of the genes encoding proteins down-regulated in hT-RPE was significantly reduced also in colorectal adenomatous polyps, early tumors in which c-Myc is invariably over-expressed. These findings help to elucidate the significance of c-Myc over-expression at early stages of tumor development and uncover a remarkable autocrine/paracrine component in the ability of c-Myc to stimulate proliferation, sustain tumor maintenance and modulate cell migration.

DOI: https://doi.org/10.1021/pr200584y

DOI: https://doi.org/10.1021/pr200584y

Article

Analysis of secretome changes uncovers an autocrine/paracrine component in the ability of c -Myc to modulate cell proliferation and motility

Gabriella Pocsfalvi, Giuseppina Votta, Anna De Vincenzo, Immacolata Fiume, Delfin Albert Amal Raj, Giancarlo Marra, Maria Patrizia Stoppelli, and Ingram Iaccarino

J. Proteome Res., **Just Accepted Manuscript** • DOI: 10.1021/pr200584y • Publication Date (Web): 20 Oct 2011

Analysis of secretome changes uncovers an autocrine/paracrine component in the modulation of cell proliferation and motility by c-Myc

Gabriella Pocsfalvi[1], Giuseppina Votta[2], Anna De Vincenzo[2], Immacolata Fiume[1], Delfin Albert Amal Raj[1], Giancarlo Marra[3], Maria Patrizia Stoppelli[2] and Ingram Iaccarino[2]*

[1] Institute of Protein Biochemistry – CNR, Via P. Castellino 111, 80131 Naples, Italy

[2] Institute of Genetics and Biophysics – CNR, Via P.Castellino 111, 80131 Naples, Italy

[3] Institute of Molecular Cancer Research, University of Zurich, Winterthurerstr. 190, CH-8057 Zurich, Switzerland

*To whom correspondence should be addressed: Ingram Iaccarino, Institute of Genetics and Biophysics – CNR, Via P.Castellino 111, 80131 Naples, Italy. Tel. +39 0816132449, Fax: +39 0816132720; e-mail: ingram.iaccarino@igb.cnr.it

Running title: Changes in the secretome induced by c-Myc

Abstract

Proteins secreted by cancer cells are a major component of tumor microenvironment. However, little is known on the impact of single oncogenic lesions on the expression of secreted proteins at early stages of tumor development. Because c-Myc over-expression is among the most frequent alterations in cancer, here we investigated the effect of sustained c-Myc expression on the secretome of a non-transformed human epithelial cell line (hT-RPE). By using a quantitative proteomic approach we have identified 125 proteins in conditioned media of hT-RPE/MycER cells upon c-Myc induction. Analysis of the 49 proteins significantly down-regulated by c-Myc, revealed a marked enrichment of factors associated with growth inhibition and cellular senescence. Accordingly, media conditioned by hT-RPE cells expressing c-Myc show an increased ability to sustain hT-RPE cellular proliferation/viability. We also find a marked down-regulation of several structural and regulatory components of the extracellular matrix (ECM), which correlates with an increased chemotactic potency of the conditioned media towards fibroblasts, a major cellular component of tumor stroma. In accordance with these data, the expression of the majority of the genes encoding proteins down-regulated in hT-RPE was significantly reduced also in colorectal adenomatous polyps, early tumors in which c-Myc is invariably over-expressed. These findings help to elucidate the significance of c-Myc over-expression at early stages of tumor development and uncover a remarkable autocrine/paracrine component in the ability of c-Myc to stimulate proliferation, sustain tumor maintenance and modulate cell migration.

Keywords

c-Myc

Secretome

c-ICAT

Oncogenic transformation

Senescence

ECM

Colorectal Cancer

Introduction

Tumor initiation and progression is a complex process where normal epithelial cells acquire a series of novel capabilities that change their behavior in the context of the tissue architecture and drive the formation of a new tissue entity: the tumor mass. The evolution of this transformation process is strictly dependent on the cellular microenvironment where it takes place and can be controlled by cell-to-cell communications of the transforming epithelial cells with the surrounding cellular components of the stroma, particularly fibroblasts, endothelial cells, macrophages and other components of the immune system[1]. Cellular communication is achieved by the ability of cells to secrete specific factors and express specific receptors on the membrane. Secreted factors can have a strong influence on tumor initiation and progression because they can mediate multiple cell-to-cell communications. They can act in an autocrine fashion by positively or negatively influencing the ability of the tumor cells to survive and/or proliferate. They can also act in a paracrine fashion by influencing the behavior of the surrounding cellular components of the stroma[2].

Autocrine production of growth and survival factors from cancer cells has long been regarded as a mechanism to uncouple cell growth and proliferation from the extracellular context[3]. Oncogenes like *ras* or *raf* are known to increase the production of the growth and survival factors, resulting in a reduced dependency on the microenvironment for growth and survival[4]. On the other hand, factors secreted by oncogenically transformed cells have been shown to mediate opposite effects on cellular physiology. Increased production of IGFBP7, for instance, has been suggested to play a major role in the induction of cellular senescence in melanocytes acquiring activating mutations in either BRAF or Ras[5]. Similarly, secreted factors like TGFβ and the inhibitors of the Wnt pathway, SRFP and DKK, are known to transduce intracellular anti-

proliferative signals and have been associated with cellular senescence[6,7]. A recent review has proposed to group the secreted factors associated to cellular senescence under the collective name of Senescence Messaging Secretome (SMS)[8].

Therefore, understanding how the pool of factors secreted by epithelial cells is influenced by the acquisition of oncogenic lesions, like the activation of oncogenes or the inactivation of tumor suppressor proteins, can be extremely useful to understand the process of tumor initiation and progression.

The transcription factor c-Myc is found over-expressed in many tumors, ranging from B-cell lymphoma to colon, breast carcinomas and melanomas[9]. A series of studies have shown that c-Myc influences the expression of a high number of proteins involved in diverse cellular functions, like cell cycle regulation, apoptosis, metabolism, cell adhesion and cellular differentiation[10]. In most cases, however, the link between the function of c-Myc target genes and the ability of this proto-oncogene to contribute to cellular transformation remains elusive. Although c-Myc can display intrinsic tumor suppressing activity when expressed in primary cells[11], c-Myc can be also required to counteract the intrinsic tumor suppressor activities of other oncogenes. In melanoma, for instance, continuous c-Myc expression is required to overcome cellular senescence induced by activating mutations in either BRAF or Ras[12]. *In vivo*, inhibition of c-Myc activity in Kras-induced tumors, using an inducible dominant negative protein, resulted in a marked shrinkage of the tumor, accompanied by a significant increase in expression of the Senescence-Associated β-Galactosidase[13]. c-Myc expression is therefore continuously required for tumor progression and maintenance.

Given the importance of c-Myc in so many aspects of cellular physiology and given the complex output resulting from c-Myc induction, a big effort has been put in the identification of c-Myc-induced transcriptional[14] and proteomic changes[15-17]. In these studies, the expression changes measured at the protein level were in good agreement with global RNA expression analyses confirming that c-Myc influences the expression of a high number of proteins involved in diverse cellular functions. Furthermore, proteomics is more effective in the analysis of specific sub-cellular compartments, making it easier to detect changes directly relevant to cellular physiology compared to global studies. On this basis, the group of Aebersold has applied a quantitative proteomics approach to characterize c-Myc induced changes in the chromatin enriched[16], soluble and mitochondrial fractions[17] of Rat1 fibroblasts.

To gain insights into the initial steps of oncogenic transformation, we have recently introduced MycER in a human epithelial cell line immortalized with the catalytic subunit of Telomerase (hT-RPE). Using this system we found that c-Myc induced the down-regulation of the secreted protease urokinase. Interestingly, this correlated with changed chemotactic properties of culture media conditioned by cells with active c-Myc[11]. This suggests that c-Myc activation could influence the microenvironment of a developing tumor, by controlling the expression of secreted proteins acting either in an autocrine or a paracrine fashion. The relevance of paracrine effects of c-Myc activation was underlined also by the work of Dews et al., showing that c-Myc-mediated repression of the anti-angiogenic factors thrombospondin-1 and CTGF resulted in vigorous tumor vascularization and growth[18]. Furthermore, in SV-40 driven tumors, c-Myc has been shown to be necessary also for the maintenance of the tumor microenvironment[19]. But how and to what extent the cellular microenvironment is altered through the regulation of the expression of secreted proteins by c-Myc has not been addressed. Therefore, we aimed to investigate c-Myc

induced changes in the entire secretome using our non-transformed epithelial cells as model system. By using a quantitative proteomic approach based on stable isotope labeling, we found that c-Myc activation resulted in the down-modulation of proteins involved in cellular senescence as well as in regulatory and structural extracellular matrix components.

Materials and Methods

Cell Culture

hT-RPE/MycER cells were described previously[11]. hT-RPE/MycER cells, parental hT-RPE cells and Swiss-3T3 mouse fibroblasts were all cultured in Dulbecco's modified Eagle's medium supplemented with 100 µg/ml streptomycin, 100 units/ml penicillin, and 10% fetal bovine serum (FBS) (pH 7.2–7.4) in a humidified atmosphere containing 5% CO_2 at 37 °C.

Sample preparation

hT-RPE/MycER cells were plated in 12 x 15 cm^2 dishes (6 x 10^5 cells/dish) and grown 48 hours in the absence (6 dishes) or the presence (6 dishes) of 150 nM 4-hydroxytamoxifene (4-OHT) in DMEM supplemented with 10% FBS. Cells were washed 7 times with 13 ml of serum-free DMEM and grown for 24 hours in serum-free DMEM with or without 150 nM 4-OHT. Conditioned media (100 ml) were collected and centrifuged 10 min at 1500 rpm to remove cell debris. Samples were concentrated using centrifugal filters with a 10 kDa cut-off (Centricon Plus-70 and Microcon, Millipore) at 4 °C. Concentrated samples were resuspended in 50 mM Tris/HCl, 0.1 % SDS, pH 8.5. Protein concentrations were determined using Micro BCA Protein Assay Kit (Thermo Scientific) and 100 µg of each sample was used for the quantitative proteomic analysis. A total of two biological samples were prepared and analyzed.

Cellular proliferation/viability assay

Cellular proliferation/viability was assayed using a Cell-Titer-Glo® Luminescent Cell Viability Assay (Promega), that measures intracellular ATP level. Briefly, equal numbers of cells (4 x 10^3

cells/well) were seeded in white-walled 96 well plates and incubated in triplicate with conditioned media (50 µl/well) from hT-RPE/MycER cells grown either in presence or in absence of 4-OHT, as described below (sample preparation). After 48 hours, a volume of 50 µl of the reaction reagent was added to each well, and after 10 min, the luminescence signal was detected using a plate-reading luminometer (GloMax® 96 Luminometer, Promega).

Chemotaxis assay

Chemotaxis assays were performed in Boyden chambers by using 8 µm-pore-size PVPF-free filters (insert growth area 0.33 cm^2) coated with collagen type VI 50 µg/ml O.N. at 4 °C, as previously described[11]. Briefly, following a 48 hours pre-incubation with or without 4-OHT in full serum medium, media conditioned by hT-RPE/MycER cells treated or not with 4-OHT for 24 hours in serum free conditions were used as chemoattractants in the lower compartment of Boyden chambers. Swiss-3T3 mouse fibroblasts were detached by mild trypsinization, and inoculated into the upper compartment of Boyden chambers. After 2h of incubation at 37°C, the cells on the upper side of the membrane were removed by scraping and cells on the lower side of the filters were stained with Ematoxilin (Mayer's) and counted.

Western Blot Analysis

Equal amounts of concentrated conditioned media were separated on a 10% SDS-PAGE and transferred to an Immobilon-P PVDF membrane (Millipore). The membrane was subsequently incubated for 2 h at room temperature in TBST buffer (125 mM Tris-HCl (pH 8.0), 625 mM NaCl, 0.1% Tween 20) containing 5% skim milk and further incubated with the primary antibodies. The immune complexes were detected using the ECL detection system, according to

the manufacturer's protocol (Millipore). Mouse monoclonal antibody anti-IGFBP-7 (W18R), rabbit polyclonal antibody anti-IGFBP-6 (H-70) and goat polyclonal antibody anti-Cathepsin D (R-20) were from Santa Cruz Biotechnology. Goat polyclonal antibody anti-Dkk3 (ab2459), mouse monoclonal antibodies anti-TGFβ2 (Ab36495) and anti-GAPDH (Ab36495) were from Abcam. Mouse monoclonal antibody anti-vimentin (V 6630) and rabbit polyclonal antibody anti-Actin were from Sigma. Rabbit polyclonal anti-uPA was a gift of P.A. Andreasen, Aarhus, Denmark.

c-ICAT labeling and sample analysis

1D PAGE cleavable ICAT (c-ICAT) procedure was performed using the c-ICAT reagent kit (Applied Biosystems) according to manufacturer's protocol with minor modifications. The two biological replicates were analyzed separately. Briefly, for each biological sample100 µg of proteins were dissolved in 80 µl 50 mM Tris 0.1% SDS and reduced with 2 µl of 50 mM TCEP for 10 min at 100 °C. Samples from control and MycER activated cells were labeled respectively with the light and heavy reagents. Samples were combined, concentrated, loaded onto 1D-SDS PAGE (1.5 mm X 10 cm) and stained with Coomassie brilliant blue G-250. The gel lane was cut into 15 slices (3-mm each) washed and in-gel digested using trypsin at 6 ng/µL in 50 mM NH_4HCO_3 10% ACN for 16 hours. Peptides were extracted sequentially using 100 µl 30% ACN 3.5% formic acid (HCOOH), 100 µl 50% ACN 5% HCOOH and 100 µl ACN, were combined and vacuum dried. Affinity chromatography by avidin cartridge was used to purify peptides. Labeled peptides were eluted in 30% ACN 0.4% TFA. The cleavable biotin group was removed by acid hydrolysis.

Samples were analyzed by nano-HPLC-ESI-MS/MS using the QSTAR Elite (Applied Biosystems, Foster City, CA, USA) equipped with a nanoflow electrospray ion source. Pulled silica capillary (170 μm OD/100 μm ID, tip 30 μm ID) was used as nanoflow tip. The samples (20 μL) were loaded, purified and concentrated on a trap column PepMap, C18, 5 mm length, 300 Å, (LCPackings, Sunnyvale, CA, USA) at 30 μL/min flow rate. Peptide separation was performed by Ultimate 3000 (Dionex, Sunnyvale, CA USA) using a capillary column, PepMap, C18, 15 cm length, 75 μm ID, 300 Å (LCPackings, Sunnyvale, CA USA), solvent A: 2% ACN in 0.1% HCOOH and solvent B: 98% ACN in 0.1% HCOOH at 300 nL/min flow rate. The following gradient was used: 5-50% B in 60 min, 50-98% B in 6 sec. CID experiments were carried out in IDA mode using nitrogen as collision gas. Two independent nano-HPLC-ESI-MS/MS experiments were performed for each sample.

Database search

Tandem mass spectra were extracted and peak lists were generated by Analyst QS 2.0 software using the default parameters. Peak lists containing all acquired MS/MS spectra were analyzed using Mascot Server (version 2.2) and X! Tandem (www.thegpm.org; version 2007.01.01.1). Mascot Server was set up to search the SwissProt 2010_09 Human database containing 20359 entries. Trypsin was specified as the digestion enzyme with a maximum of one missed cleavage site. X! Tandem was set up to search the same database. Mascot and X! Tandem were run with a fragment ion mass tolerance of 0.08 Da and a parent ion tolerance of 50 ppm. Alkylation of cysteine with ^{12}C (light) c-ICAT and with ^{13}C (heavy) c-ICAT and oxidation of methionine were set as variable modification in Mascot and X! Tandem searches.

Criteria for protein identification

Scaffold (version Scaffold_2_04_00, Proteome Software Inc., Portland, OR) was used to validate MS/MS based peptide and protein identifications. Protein probabilities were assigned by the Protein Prophet algorithm[20]. Protein identifications were accepted if they had greater than 99.0% probability and contained at least 2 unique identified peptides, unless otherwise mentioned. For proteins identified on the basis of one unique peptide the following criteria were used: i) identification in both ICAT experiments, ii) Mascot MS/MS ion score greater than 25 at significance threshold $p<0.05$ (95% confidence), iii) at least three consecutive peptide fragments identified in the MS/MS spectrum and (iv) ICAT ratio changes beyond 33% of the population median. The latter criterion was used in order to include only proteins having considerably changed expression upon cMyc induction. An analysis of false-positive rate of the protein identifications was performed by searching all tandem mass spectra from the nano-HPLC-ESI-MS/MS analyses of the c-ICAT peptide fractions against an in-house curated decoy SwissProt human protein database containing forward and reversed sequences. In addition, contaminants such as human keratins and porcine trypsin etc. were included in this database. The false-positive rate analysis resulted in the identification of 11 unique peptides from the decoy database as compared with 695 peptides from the target database. False discovery rate was calculated by computing the ratio of these two values[21]. Based on this calculation we estimate a percentage of false-positives 1.58% for the present c-ICAT peptide data set.

Quantification and Bioinformatics Analysis

All spectra (Analyst wiff file) and MASCOT-based sequence assignments were imported into the MSQuant 2.0a81software[22] for protein quantitation. MSQuant calculated the intensity ratios of

each of the heavy (H) and light (L) peptide pairs (ratio=Intensity H/Intensity L). The overall mean and variance for each peptide was determined from all observations of a given peptide at a specific time point. Final protein quantitation rations were calculated in each biological sample as the average H/L ratios of the peptides constituting the protein. All assignments made for quantitation were displayed and manually validated. Global median normalization method was used to correct for unequal mixing, labeling and for the error in the initial protein concentrations. Corrected protein ratios of the two experiments were $\log_2$ transformed and graphed on a scatter plot to visualize the biological reproducibility. Non-linear (Gaussian) regression analysis was performed using the GraphPad Prism 5 software to obtain the mean and standard deviation values of the Gaussian curve. Normal density function of Microsoft Excel was used to calculate the P values and to determine the -fold changes across the whole data set. Final protein quantitation ratios were determined by calculating the average value from the ratios of single measurements. Typical c-ICAT quantification accuracy using the above workflow was evaluated by using Bovine serum albumin standard at three different mixing ratios. Analytical coefficient of variation values was less than 10%.

Prediction tools

Secretion predictions were analyzed using the SignalP 3.0[23], SecretomeP 2.0[24] and SecretP[25] software. SignalP 3.0 and SecretomeP 2.0 were run at the Center of Biological Sequence analysis, publicly available prediction server http://www.cbs.dtu.dk/services/. SecretP was run at http://cic.scu.edu.cn/bioinformatics/secretp/index.htm. Functional annotation analysis was performed using the “Ingenuity Pathway Analysis” software.

Gene expression analysis

Gene expression analysis was carried on 34 normal colon mucosa samples and 34 colon adenomas samples using the Affymetrix U133 Plus 2.0 platform as described in Sabates-Bellver et al.[26] (GEO series record GSE8671).

Results and Discussion

Secretome analysis of hT-RPE/MycER cells

To investigate how the over-expression of the c-Myc oncoprotein could impact the secretome of non-transformed epithelial cells, we made use of hT-RPE/MycER cells, a human epithelial cell line immortalized with the catalytic subunit of Telomerase (hT-RPE) expressing a form of c-Myc (MycER) that can be activated by the addition of 4-hydroxytamoxifene (4-OHT)[11]. Changes in the secretome induced by c-Myc were analyzed using a quantitative proteomic approach based on stable isotope labeling of proteins extracted from cell culture media of hT-RPE/MycER cells treated or not with 4-OHT. The experimental workflow used in this study is shown in Figure 1.

Before replacing culture media with serum-free medium, we activated c-Myc with 4-OHT in the presence of FBS for 48 hours to ensure that the changes in the secretome induced by c-Myc were strong enough to be univocally defined. Serum-free culture media conditioned by hT-RPE/MycER cells with or w/o 4-OHT were collected after 24 hours, concentrated and processed for proteomics and Western blot analysis. We have previously shown that activation of c-Myc in hT-RPE/MycER cells for 48 hours in serum-free medium results in the induction of apoptosis[11]. Given that under cell culture conditions cell lysis could be an end product of apoptosis, we investigated if c-Myc activation could lead to a cytosolic contamination of the culture media in the experimental setup of this study. Western blot analyses against two highly abundant cytosolic proteins (e.g. glyceraldehyde 3-phosphate dehydrogenase and actin) showed that culture media were not significantly contaminated by cytosolic proteins (at least in the range of sensitivity of this technique), neither in the presence nor in the absence of 4-OHT (Fig. 2). The same

conditioned media where instead highly positive for the presence of the secreted protease urokinase (uPA). The down-regulation of uPA in the experimental conditions used is in agreement with our previous findings[11] and confirms that activation of c-Myc by 4-OHT is effective (Fig. 2).

Stable isotope labeling by cleavable-Isotope Coded Affinity Tag (c-ICAT) technology has been shown to be particularly useful in secretome analyses[27,28]. In the present study we used second-generation c-ICAT containing an acid-cleavable linker and ^{13}C (H = heavy) or ^{12}C (L = light) isotopes to differentially label protein samples derived from hT-RPE/MycER cells treated or not with 4-OHT, respectively[29-31] (2 independent experiments were performed). After labeling, the two samples of each experiment were combined and proteins were separated by 1-dimensional SDS-PAGE (12% acrylamide), followed by Coomassie Brilliant Blue (R-250) staining. The entire gel lane was cut into 15 slices, and each of them was subjected to in-gel digestion, biotin affinity chromatography and nano-HPLC-ESI-MS/MS analysis, as described in the scheme presented in Fig. 1. The relative abundance of proteins was calculated using the MSQuant open source software[22]. This is illustrated in Supplementary Figure 1, which shows a typical mass spectrum of c-ICAT-labeled peptide pairs derived from the mixed inactive and active MycER samples. Details on the quantified peptides and proteins are listed in Supplementary Table 1. In this table the 125 unique proteins that were identified and quantified by MSQuant are reported. One hundred three (82%) of these proteins are predicted to be secreted by either classical and/or non classical secretion mechanisms according to SignalP[23], SecP[24] and SecretP[25] *in-silico* secretome prediction analyses. Only 22 proteins (18%) are predicted to be either cytosolic or associated with the cytoskeleton (Supplementary Table 1). Finally, because in our previous microarray analysis of hT-RPE/Vec parental cells we found only few and slight

transcriptomic changes induced by 4-OHT treatment which were not overlapping with c-Myc-induced changes[11], we are confident that also most of the proteomic changes reported here are associated with the expression of c-Myc.

Fig. 3A shows the normal distribution plotted in terms of the number of proteins as a function of binned $\log_2$ (active/inactive MycER) ratios. Non-linear regression analysis was performed to determine the mean values. The Gaussian ratio distribution curves of independent experiments are centered at the $\log_2$ ratio -1.3 (see also Supplementary Fig. 2). This negative deviation from zero indicates a significant leftward shift in data dispersion toward markedly lower H/L (i.e., c-Myc ON/c-Myc OFF) ratios and was attributed to a down-regulation of a large proportion of proteins in the secretome of c-Myc ON cells. The $\log_2$-transformed MycER active/inactive protein intensity ratios of the two independent c-ICAT experiments showed a good reproducibility of data obtained (Fig. 3B). Statistical analysis of the two biological replicates (Supplementary Tables) indicated that 2.5-fold or greater change in protein abundance of c-Myc active versus inactive cells could be considered biologically relevant and this was taken as a cut-off value.

Using these criteria (i.e. 2.5<H/L<0.4), 49 proteins were found to be significantly down-regulated and 12 significantly up-regulated following c-Myc activation (Table 1 and 2 respectively). It is interesting to note that while 45 out of 49 down-regulated proteins are predicted to be secreted by the main signal peptide dependent mechanism (Table 1), up-regulated proteins are predicted to be secreted by non-classical mechanisms (6 out of 12) or not secreted (6 out of 12) (Table 2). Secretory vesicles like exosomes were not depleted in the samples, and thus it is not surprising that some of the non-classically secreted extracellular proteins identified in this work (like filamin A, annexin 2 and actin) have been previously identified in exosome

samples and reported in the ExoCarta database. Western blot analysis of 6 of the 61 most significantly regulated proteins (CATD, TGFB2, IBP6, IBP7, DKK3 and vimentin) was performed on the conditioned media of hT-RPE/MycER cells treated or not treated with 4-OHT and is presented in Fig. 4. Western blot analysis confirmed that CATD, TGFB2, IBP6, IBP7 and DKK3 are down-regulated following c-Myc activation and that vimentin is up-regulated.

As shown in Table 2, only 12 proteins were found to be significantly up-regulated by c-Myc (having an H/L >2.5). Six of them are predicted to be non-secreted proteins, and are therefore likely to be cytosolic contaminants of the samples. The remaining six proteins up-regulated by c-Myc are predicted to be secreted by a non-classical secretion pathway. One of them, vimentin, is a well-known intermediate filament protein, but recent studies have shown that it is secreted by macrophages in response to pro-inflammatory signaling pathways[32]. Secreted soluble vimentin has been suggested to be a potential serological marker for small-size hepatocellular carcinoma[33]. Another c-Myc up-regulated protein, potentially secreted by a non-classical secretion pathway, is the translationally-controlled tumor protein (TCTP, 3-fold up-regulated), a protein over-expressed in cancer, with a putative anti-apoptotic activity[34]. Secretion of TCTP was shown to be facilitated by TSAP6, a p53-inducible protein[35]. Increased levels of TCTP in conditioned media of hT-RPE/MycER cells could therefore be mediated by the strong up-regulation of p53 observed in this cellular system following c-Myc activation[11].

As mentioned above, almost all proteins down-regulated by c-Myc are predicted to be proteins secreted through the signal peptide dependent mechanism (Table 1). To have a general picture of the biological processes influenced by c-Myc activation, we analyzed the list of down-regulated proteins using the Ingenuity Pathway Analysis platform. The analysis shows that "Cancer" is by far the disease process most significantly associated with the 49 proteins down-

regulated upon c-Myc activation (Fig. 5A). This is interesting because the model system used in this work is not an established cancer cell line, but an immortalized epithelial cell line in which the process of oncogenic activation was mimicked by the expression of an activatable form of c-Myc. The result of this analysis also shows that the top molecular and cellular functions associated with this set of proteins are: “Cellular Movement”, “Cellular Growth and Proliferation”, “Cell-To-Cell Signaling and Interaction” and “Cell Death” (Fig. 5B). Strikingly, these are the biological functions known to be regulated by c-Myc during oncogenic transformation[10]. We also performed a manual and extensive literature search for each of the down-regulated proteins presented in Table 1, to pinpoint the cellular function(s) that would be most affected by c-Myc activation. In line with results of the Ingenuity Pathway analysis, we found that about 25% of the proteins could be positively associated to growth inhibition and/or induction of cellular senescence, and an additional 25% of them could be associated with formation or modulation of the extracellular matrix (ECM). Both senescence and ECM interaction are believed to act as strong barriers to tumor progression[36,37]. The finding that c-Myc induces a marked reduction in secreted proteins belonging to these two functional categories, suggests that inhibition of cellular senescence and ECM remodeling may play a major role in early stage c-Myc induced oncogenesis. The proteins belonging to these two functional categories and their relevance to the process of oncogenic transformation are therefore discussed in more details.

Secreted proteins with anti-proliferative/pro-senescence activity

Cellular senescence is an irreversible cell cycle arrest triggered by telomere shortening as well as a variety of cellular stresses including the activation and/or inactivation of some

oncogenes[38-40]. Given that senescence acts as a potent barrier to tumor development, proteins mediating cellular senescence are expected to play important roles in tumorigenesis. Several secreted proteins have been proposed to contribute to the establishment of senescence[8,41]. Among them insulin-like growth factor (IGF) pathway related IGF-binding protein 6 (IBP6, with gene name IGFBP6) and 7 (IBP7, with gene name IGFBP7) for example play a significant role in senescence and can be considered as senescence markers. Both IGFBPs were shown to induce growth inhibition and senescence in melanocytes[5,42], in neuroblastoma cells[43] and in colorectal cancer[44]. IGFBP6 has been shown to be down-regulated by N-Myc in neuroblastoma cells[43], epigenetically silenced in gastric cancer[45] and strongly down-regulated in the secretome of ovarian cancer cell lines compared to normal epithelia[46]. In our analysis IGFBP6 and IGFBP7 were found 7-fold and 5-fold down-regulated respectively upon c-Myc induction.

The Wnt signaling pathway is known to play a major role in growth and proliferation during tumor development. Negative regulation of the Wnt pathway has been suggested to cause cellular senescence during the early stages of both colorectal tumors and melanomas[7,47]. Inhibition of Wnt signaling can be achieved either by the down-regulation of Wnt ligands, or by regulation of secreted Wnt inhibitors belonging to the Secreted Frizzled-Related Protein (SFRP) family and/or to the Dickkopf-related (DKK) family of proteins. Interestingly, we found both SFRP1 and DKK3 strongly down-regulated by c-Myc (10 and 4 fold changes, respectively), suggesting that c-Myc could have a positive effect on the activation of the Wnt pathway. SFRP1 and the close homologue of DKK3, DKK1, have been shown to be transcriptionally repressed by c-Myc in breast cancer cells[48]. As a proof of the potential tumor suppressor role played by SFRP1 and DKK3, they were found epigenetically silenced in prostate cancer and their ectopic expression resulted in decreased proliferation[49]. DKK3 expression was found strongly reduced

also in malignant melanoma, but, in contrast to DKK1, its transcriptional repression did not involve promoter methylation, leaving space for transcription factors-mediated repression[50].

The TGFβ pathway has also been associated to inhibition of cell growth. c-Myc induced a marked down-regulation of TGFβ2 (TGFB2, 3.5-fold down regulated) (Table 1). The ability of c-Myc to bind Miz1 was shown to be important for the repression of TGFβ2 and to antagonize growth suppression and induction of senescence by TGFβ during lymphomagenesis[6]. Therefore, repression of TGFβ2 by c-Myc may be mediated by Miz1 and could play an important role in cancer progression. We also found a strong down-regulation of Follistatin-like protein 1 and 3. Although the function of these two proteins has not been univocally defined, FSTL1 was described to be positively modulated by TGFβ1 and to have tumor suppressor effects in human lung cancer cell lines[51] and in ovarian and endometrial carcinogenesis[52].

Following c-Myc activation we also observed a strong down-regulation of some secreted proteases, like Cathepsins (CATB, 14.3-fold down regulated; CATD, 11-fold down-regulated; CATL1, 6-fold down-regulated) and Metalloproteases and their inhibitors (MMP2, 8-fold down-regulated; TIMP2, 10-fold down-regulated; TIMP1, 4-fold down-regulated). Expression of both Metalloproteases and Cathepsins is known to increase during cancer progression, and to correlate to invasion and metastasis[53]. However, their expression was also found to correlate with the induction of senescence. Cathepsin D, for instance, has been proposed as promising marker of cellular senescence in several cancer cell lines treated with ionizing radiation[54]. Increased level of Cathepsin D was also observed during megakaryocytic maturation induced by thrombopoietin, a senescence-like cell-cycle arrest process[55]. The metalloprotease MMP2 and the metalloprotease inhibitor TIMP1 are also associated to senescence and are part of the Senescence-Associated Secretory Phenotypes signature both in human and mouse cells[56].

Taken together, activation of c-Myc in hT-RPE/MycER cells induces a strong reduction in the conditioned media of proteins with a known or putative anti-proliferative/pro-senescence activity. Based on this observation, we analyzed culture media conditioned by hT-RPE/MycER cells with active or inactive c-Myc for their ability to sustain proliferation of parental hT-RPE, as a measure of autocrine effects of c-Myc activation. Cellular proliferation/viability was assessed measuring intracellular ATP content. The result is presented in Fig. 6A and shows that media conditioned by cells exposed to 4-OHT exhibit an increased ability to sustain proliferation/viability of hT-RPE cells, compared to control cells. It is tempting to speculate that the observed c-Myc ability to stimulate proliferation/viability in an autocrine manner could be mediated by the reduction in anti-proliferative proteins observed in our quantitative proteomic analysis.

Secreted proteins associated to the ECM

Twenty-five percent of the proteins down-regulated by c-Myc in our secretome study (Table 1) are structurally or functionally associated to the extracellular matrix (ECM). Some of them are structural ECM or basement membrane (BM) proteins, like Biglycan (PGS1), Versican core protein (CSPG2), Laminin β (LAMB1) and Fibrillin-1 (FBN1) or cell surface molecules binding to the ECM or/and the BM, like Dystroglycan (DAG1) or Glypican-1 (GPC1). Others are supposed to be modulators of ECM function (ECM1, CCBE1, PXDN and CYR61). We also find down-regulated upon c-Myc activation the acetylglucosaminyltransferase responsible for glycan synthesis (B3GN1). Interestingly, B3GN1 was found down-regulated in prostate cancer resulting in a decreased interaction between epithelial cells and the BM[57]. c-Myc was already shown to repress the transcription of several genes controlling adhesion to the ECM[58]. Our data

complement this observation showing that also the soluble structural components of the ECM are regulated by c-Myc. The ECM has an extremely important role in epithelium development and tissue organization. Recognition and binding to the ECM by epithelial cells triggers survival signals and helps maintaining a differentiated status[2,59]. Therefore, reduction in ECM deposition by c-Myc expressing cells may be seen as a tissue remodeling event, potentially able to disrupt the normal tissue organization and start a new tissutal entity. Interestingly, structural rearrangements in ECM may also affect paracrine cellular signaling. It has been shown for instance that PGS1 can influence BMP4 morphogenetic gradients during early development[60]. ECM remodeling could affect tumor-stroma cross-talk also by creating a better substrate for stroma adhesion and a qualitative change in ECM could affect stroma recruitment by changing its chemoattractant ability. siRNA-mediated knockdown of the ECM protein CCBE1 in ovarian cancer cell lines was shown to enhanced cell migration. Accordingly CCBE1 was found frequently inactivated in ovarian cancer[61]. We found CCBE1 more than 6 times down-regulated by c-Myc in our secretome analysis (Table 1).

Therefore, reduction in ECM deposition can be associated with a change in the chemotactic properties of the cells. We have previously reported that media conditioned by hT-RPE/MycER cells after c-Myc activation have a reduced chemotactic activity on parental hT-RPE cells[11]. We now asked whether the same media could influence cellular motility in a paracrine fashion, using mouse 3T3 fibroblasts as a surrogate of an abundant stroma cell type. Interestingly, as shown in Fig. 6B, we found that media conditioned by cells with c-Myc active showed an increased chemotactic potency towards 3T3 fibroblasts relative to media from cells with c-Myc inactive. Therefore, the secretome changes induced by c-Myc result in the increased ability to

chemoattract fibroblasts, suggesting that *in vivo* c-Myc over-expression may change the cross-talk between tumor epithelial cells and fibroblast-like stroma cells.

Gene expression analysis of c-Myc down-regulated proteins in colon adenoma specimens

Since the functional annotation analysis shown in Fig. 7 suggests that the secretome changes we observed following c-Myc activation are relevant to cancer research, we sought to verify whether the 49 down-regulated factors identified in our analysis were also down-regulated in c-Myc-over-expressing tumors. We took advantage of the transcriptomic analysis performed on 32 samples of human colorectal adenomas and matched samples of normal mucosa from 28 patients described in Sabates-Bellver et al.[26]. The analysis is here extended to the transcriptome of 18 established colorectal cancer (CRC) cell lines. As expected, in both adenomas and CRC cell lines there is a strong up-regulation of the gene coding for c-Myc (Supplementary Fig. 3). Of the 49 genes coding for the proteins down-regulated by c-Myc in our secretome analysis, 41 were found expressed by the normal tissue and therefore further considered in the analysis. Twenty-seven of them (65%) were down-regulated at various degree in all the adenomas (Fig. 7 A, B); 24 genes (58%) were down-regulated at various degree in all the CRC cell lines (Fig. 7 A, B); 30 genes (73%) were down-regulated either in adenomas or in CRC cell lines (Fig. 7 A, B) and only 11 (27%) were either not regulated or up-regulated in both adenomas and CRC cell lines (Fig. 7 C). Given that cancer cell lines are usually derived from invasive tumors, we postulate that the genes belonging to the second group (Fig 7 B) may have different roles during the course of cancer progression. It is worth noticing that TGFB2, a protein known to play a tumor suppressor role in early tumorigenesis and an oncogenic role in late tumorigenesis, belongs to this group. Therefore, the secretome analysis carried out with our epithelial cellular model of oncogenic

transformation let us identify a set of secreted factors that are likely to play crucial roles during early colorectal tumorigenesis, i.e., the adenomatous stage.

Conclusions

We performed a quantitative analysis of the secretome of epithelial cells in which the expression of c-Myc was induced. Being our cells non-transformed, this induction likely represents the only oncogenic event in these cells, mimicking therefore early stages of epithelial tumorigenesis. The expression of c-Myc was accompanied by a dramatic down-regulation of ~50 proteins that appear to mediate autocrine and paracrine, anti-proliferative and pro-senescence effects. These findings are particularly interesting in the view of the fact that over-expression of c-Myc has been shown to be continuously required to release the tumorigenic barrier often operating in early tumor lesions. Also, numerous proteins associated to the ECM were down-regulated by c-Myc, a finding that should be better explored to understand the effects of c-Myc expression on cell adhesion and motility.

The relevance of our findings in the context of early tumor progression is supported by the observation that the expression of most of the factors identified in the secretome is markedly down-regulated also in colorectal adenomas, one of the most frequent preinvasive lesions detected in humans, and in which c-Myc is invariably overexpressed. We postulate that, in early stages of tumorigenesis, c-Myc sustains cell proliferation and overcomes senescence also by virtue of autocrine and paracrine mechanisms. This phenomenon, accompanied by ECM remodeling events, could favor the release of epithelial cells from the constraints given by the normal-tissue (i.e., colorectal mucosa) homeostasis and change the stromal microenvironment.

Acknowledgment

This work was supported by grants from the Association for International Cancer Research (AICR), the European Science Foundation (ESF), Eurocore Network on Membrane Architecture and Dynamics, Contract n.LSHC-CT-2003-503297, to M.P.S. and the Swiss National Science Foundation (no. 31003A-122186) to G.M.

We thank Diego L. Medina of the Telethon Institute of Genetics and Medicine for providing the antibody against Cathepsin D. We also thank Nadine Hornig and Pasquale Verde and for critical reading of the manuscript.

Supporting Information Available

Supplementary Table 1, results at the single peptide level measured upon c-Myc activation in the c-ICAT experiments. Supplementary Table 2, results at the protein level measured upon c-Myc activation in the c-ICAT experiments. Supplementary Table 3, prediction of secretion. For the prediction of classically secreted proteins (Sec SP), non-classically secreted proteins (NCSec) and non secreted proteins (NS) SignalP 3.0, SecretomeP 2.0 and SecretP software were used. Supplementary Fig. 1. Typical MS spectrum of c-ICAT-labeled peptide pairs. Supplementary Fig. 2, statistical distribution of the c-ICAT data of experiment 2. Supplementary Fig. 3, expression analysis of the c-Myc gene in normal colon mucosa, colon adenomas and CRC cell lines. This material is available free of charge via the Internet at http://pubs.acs.org.

Figures legend

Fig. 1. Experimental workflow. The diagram shows how c-Myc was activated in hT-RPE-MycER cells and how the exoprotein samples were prepared. After concentration, the samples were labeled with the c-ICAT reagent carrying either light (^{12}C) or heavy (^{13}C) carbon and resolved by SDS-PAGE. Proteins were subjected to *in-gel* proteolysis, affinity purification and the resulting peptides were identified and quantified through the steps indicated in the scheme.

Fig. 2. Activation of c-Myc does not result in contamination of conditioned media with cytosolic proteins. hT-RPE-MycER cells were grown in 10% FBS +/- 4-OHT for 48 hours. They were then shifted to serum free medium for 24 hours in presence or absence of 4-OHT. Cells and conditioned media were collected and equal amounts of extracted proteins were analysed by Western blot for the presence of a known c-Myc-regulated secreted protein (uPA) and of two highly abundant cytosolic proteins, glyceraldehyde 3-phosphate dehydrogenase (GADPH) and actin. C.M.: conditioned media.

Fig. 3. Statistical distribution of the c-ICAT data and reproducibility. (A) Normal Gaussian distribution curve fitted to experiment 1 data with mean value and standard deviation. The frequency distribution of $\log_2$ (active/inactive MycER) c-ICAT ratios was calculated and distributed into bins. The same analysis performed on experiment 2 is shown in Supplementary Fig. 2. **(B)** Comparison of the results of quantitative analysis of two biological samples. Scatter plot of $\log_2$-transformed cMycER active/inactive protein intensity ratios in two independent c-ICAT analyses of two biological samples (experiment 1 and experiment 2). Each dot represents one of the 125 unique proteins identified. Dot line is a linear y=x trendline.

Fig. 4. Immunoblot analysis on some of the proteins most significantly regulated by c-Myc. Conditioned medium from hT-RPE/MycER cells grown in the absence or presence of 4-OHT was concentrated and 2 μg of total protein for each lane was loaded onto SDS-PAGE gels. Proteins were transferred onto PVDF and probed with the indicated primary antibodies. *: aspecific band. One representative of three independent experiments is shown.

Fig. 5. Functional annotation analysis of c-Myc down-regulated extracellular proteins. The list of c-Myc down-regulated proteins shown in Table 1 was analyzed using the Ingenuity Pathway Analysis platform. Graphs A and B represent the statistical significance [indicated as – Log(p-value)] of the enrichment of proteins belonging to the "Disease and Disorders" and "Molecular and Cellular Functions" categories respectively in the set of proteins analyzed.

Fig. 6. c-Myc activation increases the ability of culture media to sustain proliferation/viability of hT-RPE cells and migration of 3T3 fibroblasts. hT-RPE-MycER cells were grown in 10% FBS for 48 hours and in serum free medium for 24 hours in absence (CM – 4-OHT) or presence (CM + 4-OHT) of 4-OHT. (**A)** Conditioned media were collected and used as culture media for parental hT-RPE. After 48 hours cellular proliferation/viability was measured using the Cell-Titer-Glo luminescent cell viability assay that measure the intracellular ATP level. The experiment was performed in triplicate and data are presented as percentage change relative to control (Cells treated with CM – 4-OHT). (**B**) Conditioned media were collected and used as chemoattractants in the lower compartment of Boyden chambers. Swiss-3T3 mouse fibroblasts (1.5 x 10^5 cells/sample) were layered in the upper chamber and incubated for 2h at 37°C. Cell migration was quantified by counting the number of cells on the lower

chamber side of the filter. The experiment was performed in triplicate and data are presented as percentage change relative to control (migration against a solution of 0.1% BSA). Significance was calculated using the Student t test. The p-values for each experiment was < 0.001.

Fig. 7. Secreted factors down-regulated by c-Myc are also down-regulated in colorectal adenomas and CRC cell lines. The expression of the genes coding for the proteins down-regulated by c-Myc activation in conditioned media of hT-RPE/MycER cells was analyzed in microarray data sets (Affymetrix U133 Plus 2.0 platform) from 34 normal colon mucosa samples, 34 colon adenomas and 18 CRC cell lines (HCT116, CO115, SW48, GP5d, LS174T, SW620, HT29, Caco2, COLO741, SW837, SW480, CX-1, LS180, LS411, COLO205, SW403, LOVO, DLD1). Data are shown as % of the mean expression values in normal mucosa samples. (**A**) Genes down-regulated in both adenomas and in CRC cell lines; (**B**) genes down-regulated either in adenomas and or in CRC cell lines; (**C**) genes up-regulated in both adenomas and in cell lines.

References

(1) Pietras, K.; Östman, A. Hallmarks of cancer: Interactions with the tumor stroma. *Experimental Cell Research* **2010**, *316*, 1324-1331.
(2) Bhowmick, N. A.; Moses, H. L. Tumor-stroma interactions. *Curr. Opin. Genet. Dev* **2005**, *15*, 97-101.
(3) Hanahan, D.; Weinberg, R. A. The hallmarks of cancer. *Cell* **2000**, *100*, 57-70.
(4) Schulze, A. Lehmann, K. Jefferies, H. B. McMahon, M.; Downward, J. Analysis of the transcriptional program induced by Raf in epithelial cells. *Genes Dev* **2001**, *15*, 981-994.
(5) Wajapeyee, N. Serra, R. W. Zhu, X. Mahalingam, M.; Green, M. R. Oncogenic BRAF induces senescence and apoptosis through pathways mediated by the secreted protein IGFBP7. *Cell* **2008**, *132*, 363-374.
(6) van Riggelen, J. Müller, J. Otto, T. Beuger, V. Yetil, A. Choi, P. S. Kosan, C. Möröy, T. Felsher, D. W.; Eilers, M. The interaction between Myc and Miz1 is required to antagonize TGFbeta-

dependent autocrine signaling during lymphoma formation and maintenance. *Genes Dev* **2010**, *24*, 1281-1294.
(7) Adams, P. D.; Enders, G. H. Wnt-signaling and senescence: A tug of war in early neoplasia? *Cancer Biol. Ther* **2008**, *7*, 1706-1711.
(8) Kuilman, T.; Peeper, D. S. Senescence-messaging secretome: SMS-ing cellular stress. *Nat. Rev. Cancer* **2009**, *9*, 81-94.
(9) Nesbit, C. E. Tersak, J. M.; Prochownik, E. V. MYC oncogenes and human neoplastic disease. *Oncogene* **1999**, *18*, 3004-3016.
(10) Eilers, M.; Eisenman, R. N. Myc's broad reach. *Genes Dev* **2008**, *22*, 2755-2766.
(11) Alfano, D. Votta, G. Schulze, A. Downward, J. Caputi, M. Stoppelli, M. P.; Iaccarino, I. Modulation of cellular migration and survival by c-Myc through the downregulation of urokinase (uPA) and uPA receptor. *Mol. Cell. Biol* **2010**, *30*, 1838-1851.
(12) Zhuang, D. Mannava, S. Grachtchouk, V. Tang, W.-H. Patil, S. Wawrzyniak, J. A. Berman, A. E. Giordano, T. J. Prochownik, E. V. Soengas, M. S.; Nikiforov, M. A. C-MYC overexpression is required for continuous suppression of oncogene-induced senescence in melanoma cells. *Oncogene* **2008**, *27*, 6623-6634.
(13) Soucek, L. Whitfield, J. Martins, C. P. Finch, A. J. Murphy, D. J. Sodir, N. M. Karnezis, A. N. Swigart, L. B. Nasi, S.; Evan, G. I. Modelling Myc inhibition as a cancer therapy. *Nature* **2008**, *455*, 679-683.
(14) Fernandez, P. C. Frank, S. R. Wang, L. Schroeder, M. Liu, S. Greene, J. Cocito, A.; Amati, B. Genomic targets of the human c-Myc protein. *Genes Dev* **2003**, *17*, 1115-1129.
(15) Shiio, Y. Donohoe, S. Yi, E. C. Goodlett, D. R. Aebersold, R.; Eisenman, R. N. Quantitative proteomic analysis of Myc oncoprotein function. *EMBO J* **2002**, *21*, 5088-5096.
(16) Shiio, Y. Eisenman, R. N. Yi, E. C. Donohoe, S. Goodlett, D. R.; Aebersold, R. Quantitative proteomic analysis of chromatin-associated factors. *J. Am. Soc. Mass Spectrom* **2003**, *14*, 696-703.
(17) Shiio, Y. Suh, K. S. Lee, H. Yuspa, S. H. Eisenman, R. N.; Aebersold, R. Quantitative proteomic analysis of myc-induced apoptosis: a direct role for Myc induction of the mitochondrial chloride ion channel, mtCLIC/CLIC4. *J. Biol. Chem* **2006**, *281*, 2750-2756.
(18) Dews, M. Homayouni, A. Yu, D. Murphy, D. Sevignani, C. Wentzel, E. Furth, E. Lee, W. Enders, G. Mendell, J.; Thomas-Tikhonenko, A. Augmentation of tumor angiogenesis by a Myc-activated microRNA cluster. *Nat. Genet.* **2006**, *38*, 1060-1065.
(19) Sodir, N. M. Swigart, L. B. Karnezis, A. N. Hanahan, D. Evan, G. I.; Soucek, L. Endogenous Myc maintains the tumor microenvironment. *Genes Dev* **2011**, *25*, 907-916.
(20) Nesvizhskii, A. I. Keller, A. Kolker, E.; Aebersold, R. A statistical model for identifying proteins by tandem mass spectrometry. *Anal. Chem* **2003**, *75*, 4646-4658.
(21) Käll, L. Storey, J. D. MacCoss, M. J.; Noble, W. S. Assigning significance to peptides identified by tandem mass spectrometry using decoy databases. *J. Proteome Res* **2008**, *7*, 29-34.
(22) Mortensen, P. Gouw, J. W. Olsen, J. V. Ong, S.-E. Rigbolt, K. T. G. Bunkenborg, J. Cox, J. Foster, L. J. Heck, A. J. R. Blagoev, B. Andersen, J. S.; Mann, M. MSQuant, an open source platform for mass spectrometry-based quantitative proteomics. *J. Proteome Res* **2010**, *9*, 393-403.
(23) Emanuelsson, O. Brunak, S. von Heijne, G.; Nielsen, H. Locating proteins in the cell using TargetP, SignalP and related tools. *Nat Protoc* **2007**, *2*, 953-971.
(24) Bendtsen, J. D. Jensen, L. J. Blom, N. Von Heijne, G.; Brunak, S. Feature-based prediction of non-classical and leaderless protein secretion. *Protein Eng. Des. Sel* **2004**, *17*, 349-356.

(25) Yu, L. Guo, Y. Zhang, Z. Li, Y. Li, M. Li, G. Xiong, W.; Zeng, Y. SecretP: a new method for predicting mammalian secreted proteins. *Peptides* **2010**, *31*, 574-578.
(26) Sabates-Bellver, J. Van der Flier, L. G. de Palo, M. Cattaneo, E. Maake, C. Rehrauer, H. Laczko, E. Kurowski, M. A. Bujnicki, J. M. Menigatti, M. Luz, J. Ranalli, T. V. Gomes, V. Pastorelli, A. Faggiani, R. Anti, M. Jiricny, J. Clevers, H.; Marra, G. Transcriptome profile of human colorectal adenomas. *Mol. Cancer Res* **2007**, *5*, 1263-1275.
(27) Khwaja, F. W. Svoboda, P. Reed, M. Pohl, J. Pyrzynska, B.; Van Meir, E. G. Proteomic identification of the wt-p53-regulated tumor cell secretome. *Oncogene* **2006**, *25*, 7650-7661.
(28) Zhou, H. Xiao, Y. Li, R. Hong, S. Li, S. Wang, L. Zeng, R.; Liao, K. Quantitative analysis of secretome from adipocytes regulated by insulin. *Acta Biochim. Biophys. Sin. (Shanghai)* **2009**, *41*, 910-921.
(29) Li, J. Steen, H.; Gygi, S. P. Protein profiling with cleavable isotope-coded affinity tag (cICAT) reagents: the yeast salinity stress response. *Mol. Cell Proteomics* **2003**, *2*, 1198-1204.
(30) Yi, E. C. Li, X.-J. Cooke, K. Lee, H. Raught, B. Page, A. Aneliunas, V. Hieter, P. Goodlett, D. R.; Aebersold, R. Increased quantitative proteome coverage with (13)C/(12)C-based, acid-cleavable isotope-coded affinity tag reagent and modified data acquisition scheme. *Proteomics* **2005**, *5*, 380-387.
(31) Vaughn, C. P. Crockett, D. K. Lim, M. S.; Elenitoba-Johnson, K. S. J. Analytical characteristics of cleavable isotope-coded affinity tag-LC-tandem mass spectrometry for quantitative proteomic studies. *J Mol Diagn* **2006**, *8*, 513-520.
(32) Mor-Vaknin, N. Punturieri, A. Sitwala, K.; Markovitz, D. M. Vimentin is secreted by activated macrophages. *Nat. Cell Biol* **2003**, *5*, 59-63.
(33) Sun, S. Poon, R. T. P. Lee, N. P. Yeung, C. Chan, K. L. Ng, I. O. L. Day, P. J. R.; Luk, J. M. Proteomics of hepatocellular carcinoma: serum vimentin as a surrogate marker for small tumors (<or=2 cm). *J. Proteome Res* **2010**, *9*, 1923-1930.
(34) Gnanasekar, M. Thirugnanam, S. Zheng, G. Chen, A.; Ramaswamy, K. Gene silencing of translationally controlled tumor protein (TCTP) by siRNA inhibits cell growth and induces apoptosis of human prostate cancer cells. *Int. J. Oncol* **2009**, *34*, 1241-1246.
(35) Amzallag, N. Passer, B. J. Allanic, D. Segura, E. Théry, C. Goud, B. Amson, R.; Telerman, A. TSAP6 facilitates the secretion of translationally controlled tumor protein/histamine-releasing factor via a nonclassical pathway. *J. Biol. Chem* **2004**, *279*, 46104-46112.
(36) Evan, G. I.; d' Adda di Fagagna, F. Cellular senescence: hot or what? *Curr. Opin. Genet. Dev* **2009**, *19*, 25-31.
(37) Reuter, J. A. Ortiz-Urda, S. Kretz, M. Garcia, J. Scholl, F. A. Pasmooij, A. M. G. Cassarino, D. Chang, H. Y.; Khavari, P. A. Modeling inducible human tissue neoplasia identifies an extracellular matrix interaction network involved in cancer progression. *Cancer Cell* **2009**, *15*, 477-488.
(38) Collado, M. Blasco, M. A.; Serrano, M. Cellular senescence in cancer and aging. *Cell* **2007**, *130*, 223-233.
(39) Dhomen, N. Reis-Filho, J. S. da Rocha Dias, S. Hayward, R. Savage, K. Delmas, V. Larue, L. Pritchard, C.; Marais, R. Oncogenic Braf Induces Melanocyte Senescence and Melanoma in Mice. *Cancer Cell* **2009**, *15*, 294-303.
(40) Wu, C.-H. van Riggelen, J. Yetil, A. Fan, A. C. Bachireddy, P.; Felsher, D. W. Cellular senescence is an important mechanism of tumor regression upon c-Myc inactivation. *Proc. Natl. Acad. Sci. U.S.A* **2007**, *104*, 13028-13033.

(41) Kuilman, T. Michaloglou, C. Mooi, W. J.; Peeper, D. S. The essence of senescence. *Genes Dev* **2010**, *24*, 2463-2479.
(42) Edmondson, S. R. Russo, V. C. McFarlane, A. C. Wraight, C. J.; Werther, G. A. Interactions between growth hormone, insulin-like growth factor I, and basic fibroblast growth factor in melanocyte growth. *J. Clin. Endocrinol. Metab* **1999**, *84*, 1638-1644.
(43) Babajko, S. Leneuve, P. Loret, C.; Binoux, M. IGF-binding protein-6 is involved in growth inhibition in SH-SY5Y human neuroblastoma cells: its production is both IGF- and cell density-dependent. *J. Endocrinol* **1997**, *152*, 221-227.
(44) Ruan, W. Xu, E. Xu, F. Ma, Y. Deng, H. Huang, Q. Lv, B. Hu, H. Lin, J. Cui, J. Di, M. Dong, J.; Lai, M. IGFBP7 plays a potential tumor suppressor role in colorectal carcinogenesis. *Cancer Biol. Ther* **2007**, *6*, 354-359.
(45) Jee, C. D. Kim, M. A. Jung, E. J. Kim, J.; Kim, W. H. Identification of genes epigenetically silenced by CpG methylation in human gastric carcinoma. *Eur. J. Cancer* **2009**, *45*, 1282-1293.
(46) Gunawardana, C. G. Kuk, C. Smith, C. R. Batruch, I. Soosaipillai, A.; Diamandis, E. P. Comprehensive analysis of conditioned media from ovarian cancer cell lines identifies novel candidate markers of epithelial ovarian cancer. *J. Proteome Res* **2009**, *8*, 4705-4713.
(47) Ye, X. Zerlanko, B. Kennedy, A. Banumathy, G. Zhang, R.; Adams, P. D. Downregulation of Wnt signaling is a trigger for formation of facultative heterochromatin and onset of cell senescence in primary human cells. *Mol. Cell* **2007**, *27*, 183-196.
(48) Cowling, V. H. D'Cruz, C. M. Chodosh, L. A.; Cole, M. D. c-Myc transforms human mammary epithelial cells through repression of the Wnt inhibitors DKK1 and SFRP1. *Mol. Cell. Biol* **2007**, *27*, 5135-5146.
(49) Lodygin, D. Epanchintsev, A. Menssen, A. Diebold, J.; Hermeking, H. Functional epigenomics identifies genes frequently silenced in prostate cancer. *Cancer Res* **2005**, *65*, 4218-4227.
(50) Kuphal, S. Lodermeyer, S. Bataille, F. Schuierer, M. Hoang, B. H.; Bosserhoff, A. K. Expression of Dickkopf genes is strongly reduced in malignant melanoma. *Oncogene* **2006**, *25*, 5027-5036.
(51) Sumitomo, K. Kurisaki, A. Yamakawa, N. Tsuchida, K. Shimizu, E. Sone, S.; Sugino, H. Expression of a TGF-beta1 inducible gene, TSC-36, causes growth inhibition in human lung cancer cell lines. *Cancer Lett* **2000**, *155*, 37-46.
(52) Chan, Q. K. Y. Ngan, H. Y. S. Ip, P. P. C. Liu, V. W. S. Xue, W. C.; Cheung, A. N. Y. Tumor suppressor effect of follistatin-like 1 in ovarian and endometrial carcinogenesis: a differential expression and functional analysis. *Carcinogenesis* **2009**, *30*, 114-121.
(53) Mohamed, M. M.; Sloane, B. F. Cysteine cathepsins: multifunctional enzymes in cancer. *Nat. Rev. Cancer* **2006**, *6*, 764-775.
(54) Byun, H.-O. Han, N.-K. Lee, H.-J. Kim, K.-B. Ko, Y.-G. Yoon, G. Lee, Y.-S. Hong, S.-I.; Lee, J.-S. Cathepsin D and eukaryotic translation elongation factor 1 as promising markers of cellular senescence. *Cancer Res* **2009**, *69*, 4638-4647.
(55) Besancenot, R. Chaligné, R. Tonetti, C. Pasquier, F. Marty, C. Lécluse, Y. Vainchenker, W. Constantinescu, S. N.; Giraudier, S. A senescence-like cell-cycle arrest occurs during megakaryocytic maturation: implications for physiological and pathological megakaryocytic proliferation. *PLoS Biol* **2010**, *8*.
(56) Coppé, J.-P. Patil, C. K. Rodier, F. Sun, Y. Muñoz, D. P. Goldstein, J. Nelson, P. S. Desprez, P.-Y.; Campisi, J. Senescence-associated secretory phenotypes reveal cell-nonautonomous functions of oncogenic RAS and the p53 tumor suppressor. *PLoS Biol* **2008**, *6*, 2853-2868.

(57) Bao, X. Kobayashi, M. Hatakeyama, S. Angata, K. Gullberg, D. Nakayama, J. Fukuda, M. N.; Fukuda, M. Tumor suppressor function of laminin-binding alpha-dystroglycan requires a distinct beta3-N-acetylglucosaminyltransferase. *Proc. Natl. Acad. Sci. U.S.A* **2009**, *106*, 12109-12114.
(58) Frye, M. Gardner, C. Li, E. R. Arnold, I.; Watt, F. M. Evidence that Myc activation depletes the epidermal stem cell compartment by modulating adhesive interactions with the local microenvironment. *Development* **2003**, *130*, 2793-2808.
(59) Frisch, S. M.; Francis, H. Disruption of epithelial cell-matrix interactions induces apoptosis. *J. Cell Biol* **1994**, *124*, 619-626.
(60) Moreno, M. Muñoz, R. Aroca, F. Labarca, M. Brandan, E.; Larraín, J. Biglycan is a new extracellular component of the Chordin-BMP4 signaling pathway. *EMBO J* **2005**, *24*, 1397-1405.
(61) Barton, C. A. Gloss, B. S. Qu, W. Statham, A. L. Hacker, N. F. Sutherland, R. L. Clark, S. J.; O'Brien, P. M. Collagen and calcium-binding EGF domains 1 is frequently inactivated in ovarian cancer by aberrant promoter hypermethylation and modulates cell migration and survival. *Br. J. Cancer* **2010**, *102*, 87-96.

Table 1. List of proteins down-regulated upon c-Myc activation.

UniProt ID	Protein UniProt Name	Fold change[a]	Mass	Secretion[b]	Exo[c]
SFRP1_HUMAN	Secreted frizzled-related protein 1	0.06	35386	Sec SP	yes
CATB_HUMAN	Cathepsin B	0.07	37822	Sec SP	yes
SEM7A_HUMAN	Semaphorin-7A	0.07	74824	Sec SP	no
CH3L1_HUMAN	Chitinase-3-like protein 1	0.08	42625	Sec SP	no
APLP2_HUMAN	Amyloid-like protein 2	0.08	86956	Sec SP	yes
ECM1_HUMAN	Extracellular matrix protein 1	0.09	60674	Sec SP	yes
CATD_HUMAN	Cathepsin D	0.09	44552	Sec SP	yes
SAP_HUMAN	Proactivator polypeptide	0.09	58113	Sec SP	yes
TIMP2_HUMAN	Metalloproteinase inhibitor 2	0.10	24399	Sec SP	no
GNS_HUMAN	N-acetylglucosamine-6-sulfatase	0.10	62082	Sec SP	no
FSTL3_HUMAN	Follistatin-related protein 3	0.11	27663	Sec SP	no
MMP2_HUMAN	72 kDa type IV collagenase	0.12	73882	Sec SP	no
MXRA8_HUMAN	Matrix-remodeling-associated protein 8	0.13	49132	Sec SP	yes
FLNA_HUMAN	Filamin-A	0.13	280739	NS	yes
IBP6_HUMAN	Insulin-like growth factor-binding protein 6	0.14	25322	Sec SP	no
PTX3_HUMAN	Pentraxin-related protein PTX3	0.15	42020	Sec SP	yes
CCBE1_HUMAN	Collagen and calcium-binding EGF domain-containing protein 1	0.15	44103	Sec SP	no
GPC1_HUMAN	Glypican-1	0.16	61650	Sec SP	yes
PGS1_HUMAN	Biglycan	0.16	41628	Sec SP	yes
TICN1_HUMAN	Testican-1	0.16	49124	Sec SP	no
CATL1_HUMAN	Cathepsin L1	0.17	37564	Sec SP	no
PTPRB_HUMAN	Receptor-type tyrosine-protein phosphatase beta	0.17	224188	Sec SP	no
UFO_HUMAN	Tyrosine-protein kinase receptor UFO	0.18	98336	Sec SP	no
B3GN1_HUMAN	N-acetyllactosaminide beta-1,3-N-acetylglucosaminyltransferase	0.19	47089	Sec SP	no
NPC2_HUMAN	Epididymal secretory protein E1	0.19	16570	Sec SP	no
FBLN1_HUMAN	Fibulin-1	0.20	77162	Sec SP	yes
SRCRL_HUMAN	Scavenger receptor cysteine-rich domain-containing protein	0.20	115770	Sec SP	no
IBP7_HUMAN	Insulin-like growth factor-binding protein 7	0.21	29130	Sec SP	no
CSPG2_HUMAN	Versican core protein	0.21	372820	Sec SP	no
ANT3_HUMAN	Antithrombin-III	0.23	52602	Sec SP	no
STC2_HUMAN	Stanniocalcin-2	0.23	33249	Sec SP	no
ANXA2_HUMAN	Annexin A2	0.24	38604	NCSec	yes
STC1_HUMAN	Stanniocalcin-1	0.24	27621	Sec SP	No
TIMP1_HUMAN	Metalloproteinase inhibitor 1	0.25	23171	Sec SP	No
DKK3_HUMAN	Dickkopf-related protein 3	0.25	38291	Sec SP	no
LAMB1_HUMAN	Laminin subunit beta-1	0.25	197937	Sec SP	no
OAF_HUMAN	Out at first protein homolog	0.26	30669	Sec SP	no
PXDN_HUMAN	Peroxidasin homolog	0.27	165170	Sec SP	no
DAG1_HUMAN	Dystroglycan	0.28	97441	Sec SP	yes
FSTL1_HUMAN	Follistatin-related protein 1	0.29	34986	Sec SP	no
TGFB2_HUMAN	Transforming growth factor beta-2	0.29	47717	Sec SP	no
KPYM_HUMAN	Pyruvate kinase isozymes M1/M2	0.30	57937	NS	yes
LIF_HUMAN	Leukemia inhibitory factor	0.30	22008	Sec SP	no
ACTA_HUMAN	Actin, aortic smooth muscle	0.31	42009	NCSec	yes
AGRIN_HUMAN	Agrin	0.33	214846	Sec SP	yes
LMAN2_HUMAN	Vesicular integral-membrane protein VIP36	0.33	40229	Sec SP	no
CYR61_HUMAN	Protein CYR61	0.34	42027	Sec SP	no
FBN1_HUMAN	Fibrillin-1	0.36	312298	Sec SP	no
CADH2_HUMAN	Cadherin-2	0.37	99809	Sec SP	no

[a]c-Myc ON/c-Myc OFF. [b]Prediction results of secretion: Sec SP,classical secretion, NCSec, non classical secretion, NS non secreted. [c]Present or not in exosomes preparations (ExoCarta database).

Table 2. List of proteins up-regulated upon c-Myc activation.

UniProt ID	Protein UniProt Name	Fold change[a]	Mass	Secretion[b]	Exo[c]
TALDO_HUMAN	Transaldolase	2.49	37540	NS	no
HNRPD_HUMAN	Heterogeneous nuclear ribonucleoprotein D0	2.61	38434	NS	no
NDKA_HUMAN	Nucleoside diphosphate kinase A	2.63	17149	NS	yes
UCHL1_HUMAN	Ubiquitin carboxyl-terminal hydrolase isozyme L1	2.66	24824	NCSec	no
PIN1_HUMAN	Peptidyl-prolyl cis-trans isomerase NIMA-interacting 1	2.79	18243	NCSec	no
RS21_HUMAN	40S ribosomal protein S21	3.02	9111	NCSec	yes
RS3A_HUMAN	40S ribosomal protein S3a	3.17	29926	NCSec	no
TCTP_HUMAN	Translationally-controlled tumor protein	3.25	19595	NCSec	no
FABP5_HUMAN	Fatty acid-binding protein, epidermal	4.97	15164	NS	no
KI26A_HUMAN	Kinesin-like protein KIF26A	6.22	194468	NS	no
VIME_HUMAN	Vimentin	6.36	53652	NCSec	no
TARA_HUMAN	TRIO and F-actin-binding protein	7.41	261217	NS	no

[a]c-Myc ON/c-Myc OFF. [b]Prediction results of secretion: Sec SP,classical secretion, NCSec, non classical secretion, NS non secreted. [c]Present or not in exosomes preparations (ExoCarta database).

Table of Contents Synopsis

We have applied a quantitative proteomics analysis to study changes in the secretome induced by the oncogene c-Myc. We found that c-Myc expression results in the down-regulation of proteins associated with growth inhibition and with the extracellular matrix. Strikingly, the expression of the majority of the proteins down-regulated by c-Myc, was significantly reduced also in colorectal adenomatous polyps, early tumors in which c-Myc is invariably over-expressed.

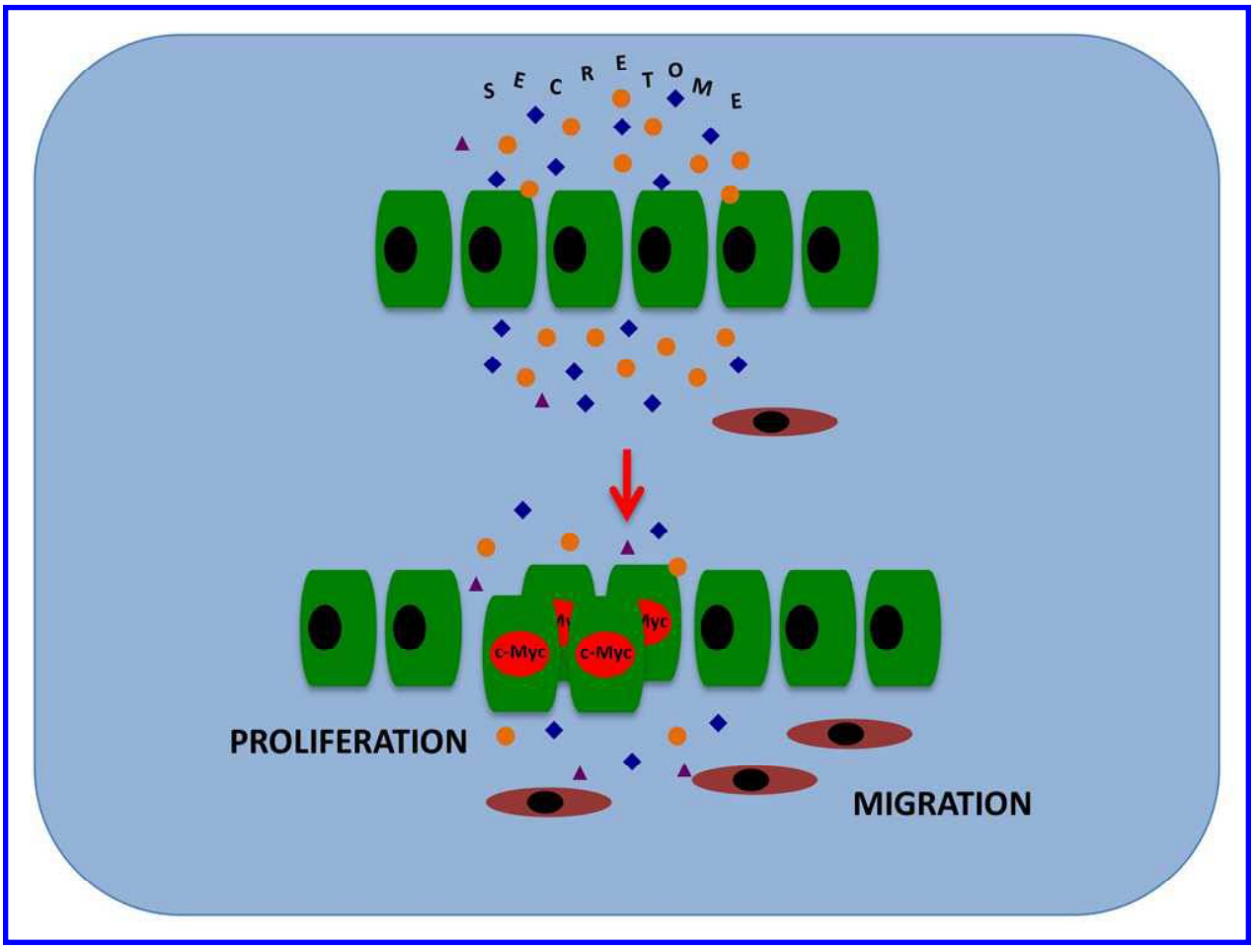

Fig. 1

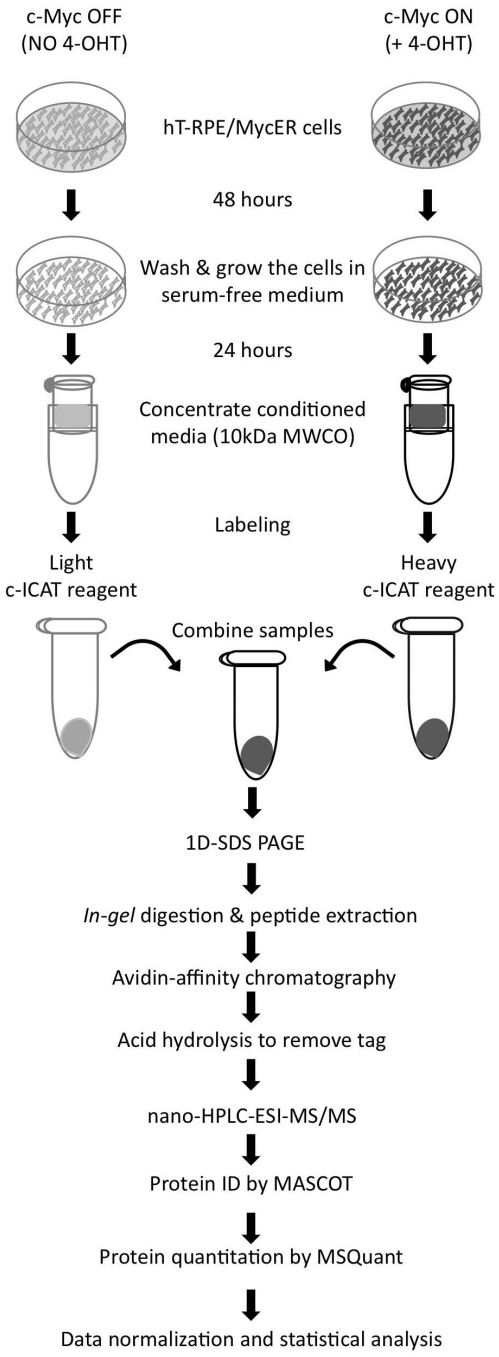
c-Myc OFF
(NO 4-OHT)
c-Myc ON
(+ 4-OHT)
hT-RPE/MycER cells
48 hours
Wash & grow the cells in serum-free medium
24 hours
Concentrate conditioned media (10kDa MWCO)
Labeling
Light c-ICAT reagent
Heavy c-ICAT reagent
Combine samples
1D-SDS PAGE
In-gel digestion & peptide extraction
Avidin-affinity chromatography
Acid hydrolysis to remove tag
nano-HPLC-ESI-MS/MS
Protein ID by MASCOT
Protein quantitation by MSQuant
Data normalization and statistical analysis

Fig. 2

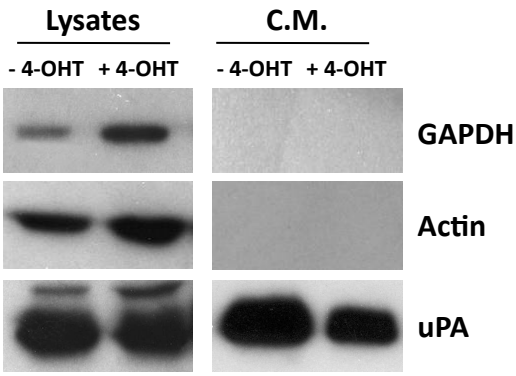

Fig. 3

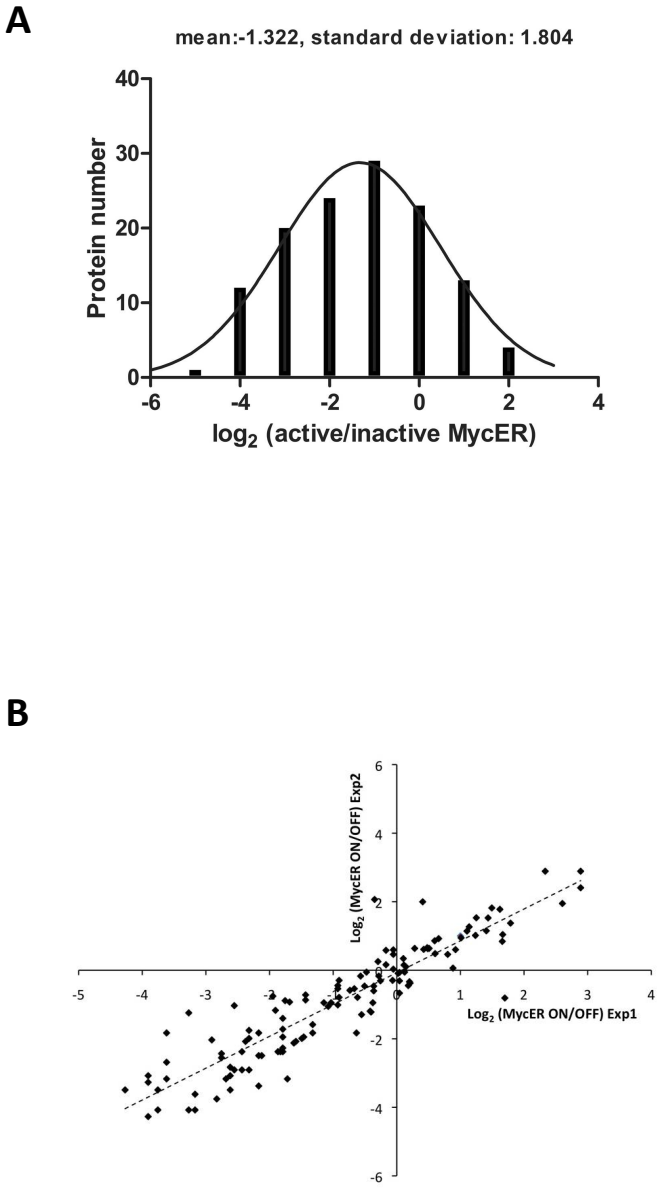
A
mean:-1.322, standard deviation: 1.804
Protein number
log2 (active/inactive MycER)
B
Log2 (MycER ON/OFF) Exp2
Log2 (MycER ON/OFF) Exp1

Fig. 4

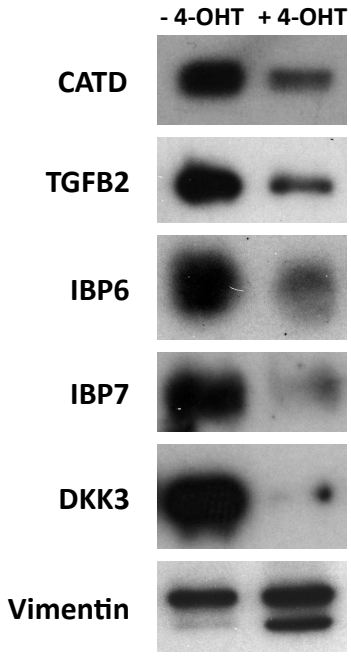

Fig. 5

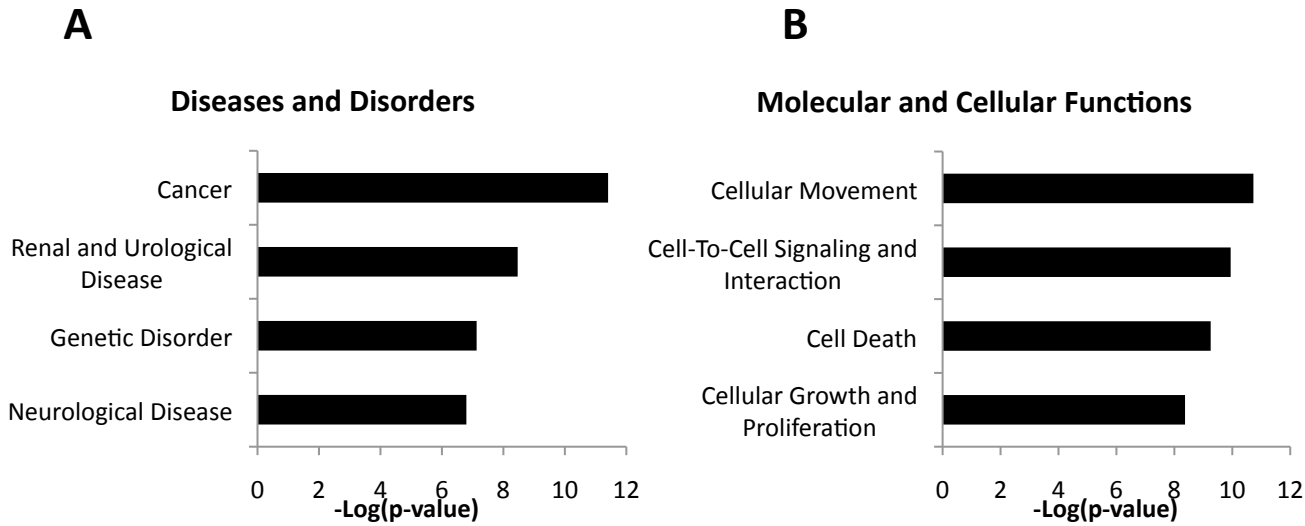
A
Diseases and Disorders
Cancer
Renal and Urological Disease
Genetic Disorder
Neurological Disease
0
2
4
6
8
10
12
-Log(p-value)
B
Molecular and Cellular Functions
Cellular Movement
Cell-To-Cell Signaling and Interaction
Cell Death
Cellular Growth and Proliferation
0
2
4
6
8
10
12
-Log(p-value)

Fig. 6

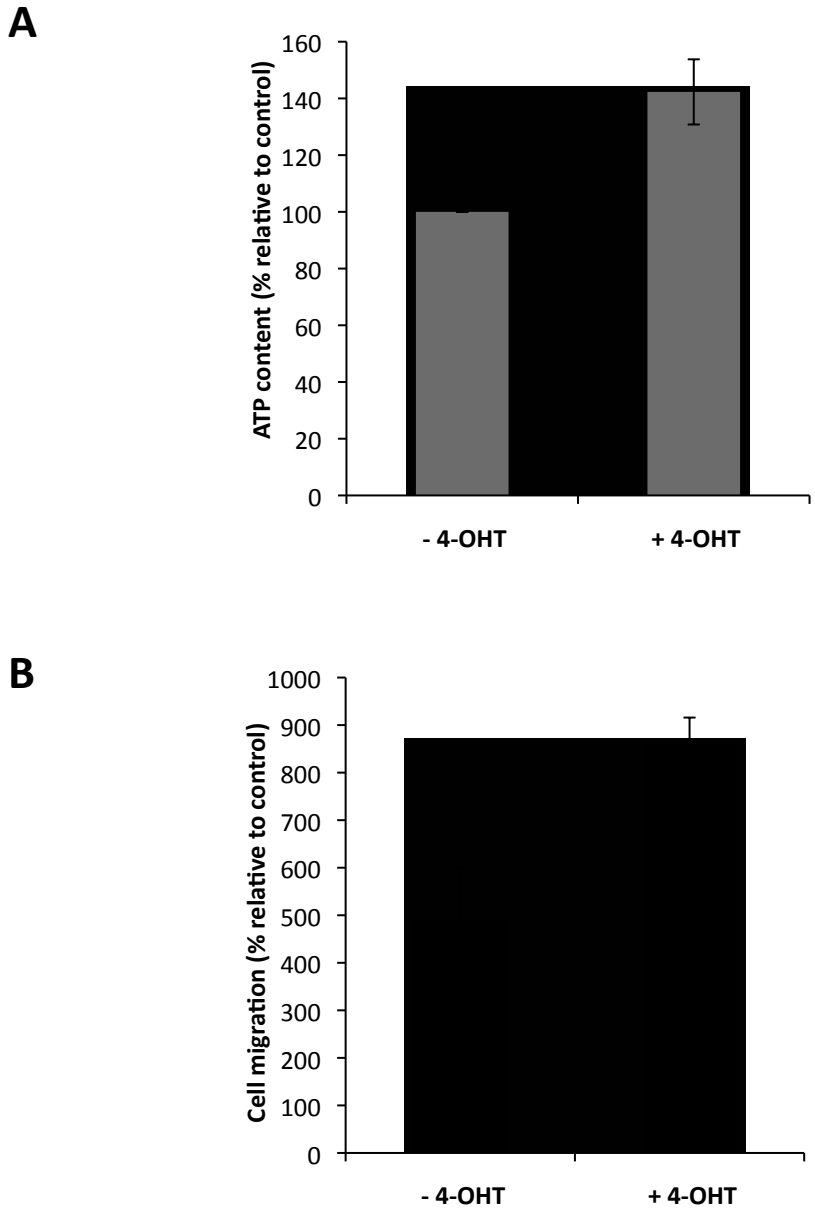
A
ATP content (% relative to control)
160
140
120
100
80
60
40
20
0
- 4-OHT
+ 4-OHT
B
Cell migration (% relative to control)
1000
900
800
700
600
500
400
300
200
100
0
- 4-OHT
+ 4-OHT

Fig. 7

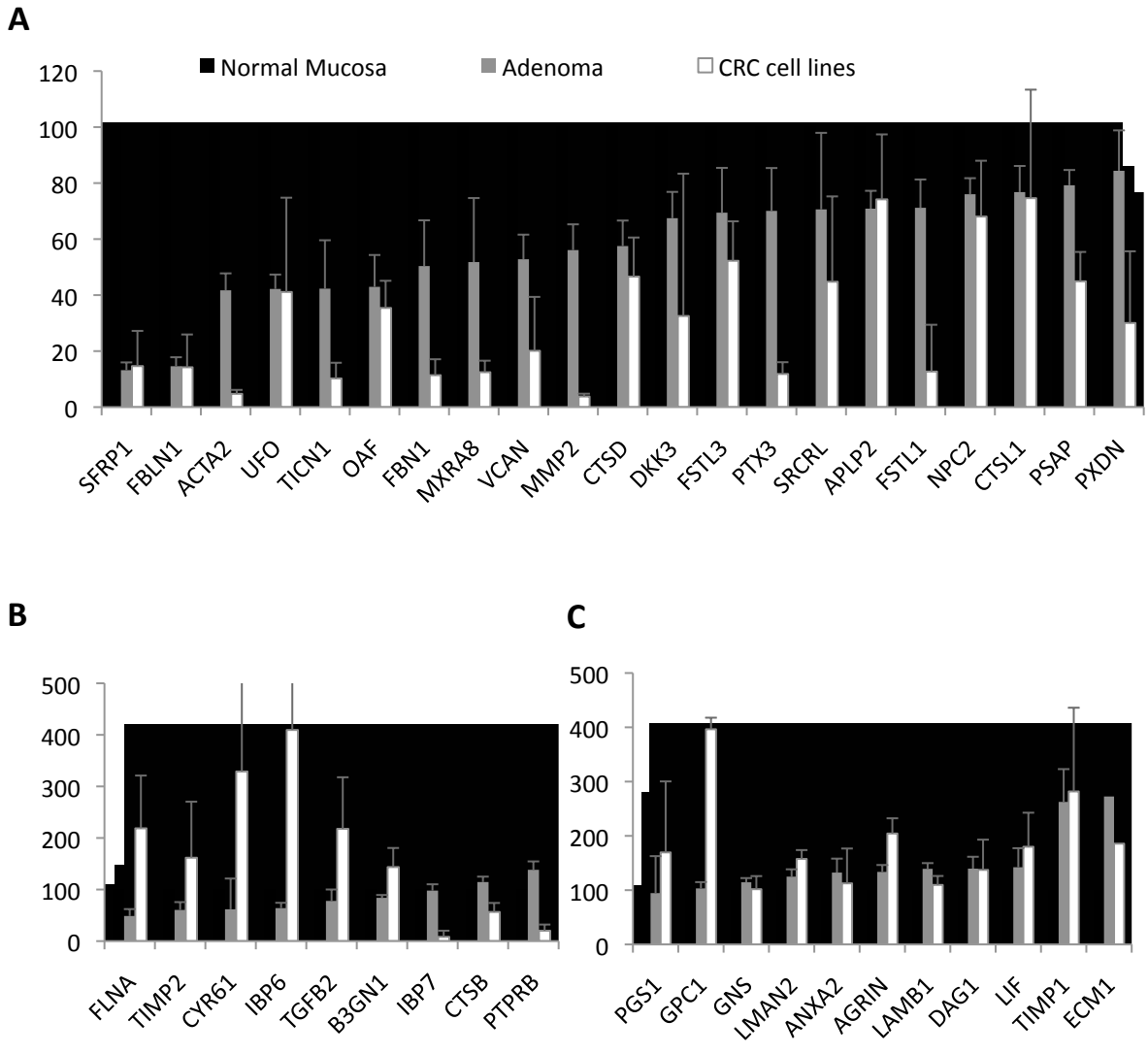
A
Normal Mucosa
Adenoma
CRC cell lines
120
100
80
60
40
20
0
SFRP1
FBLN1
ACTA2
UFO
TICN1
OAF
FBN1
MXRA8
VCAN
MMP2
CTSD
DKK3
FSTL3
PTX3
SRCRL
APLP2
FSTL1
NPC2
CTSL1
PSAP
PXDN
B
500
400
300
200
100
0
FLNA
TIMP2
CYR61
IBP6
TGFB2
B3GN1
IBP7
CTSB
PTPRB
C
500
400
300
200
100
0
PGS1
GPC1
GNS
LMAN2
ANXA2
AGRIN
LAMB1
DAG1
LIF
TIMP1
ECM1